JACS
JOURNAL OF THE AMERICAN CHEMICAL SOCIETY

pubs.acs.org/JACS

Communication

Ruthenium-Catalyzed *trans*-Hydroalkynylation and *trans*-Chloroalkynylation of Internal Alkynes

Nagaraju Barsu, Markus Leutzsch, and Alois Fürstner*

Cite This: *J. Am. Chem. Soc.* 2020, 142, 18746−18752

Read Online

ACCESS | Metrics & More | Article Recommendations | Supporting Information

ABSTRACT: $[Cp^*RuCl]_4$ catalyzes the addition of $iPr_3SiC{\equiv}CX$ (X = H, Cl) across internal alkynes with formation of 1,3-enyne or 1-chloro-1,3-enyne derivatives, respectively; the reaction follows an unorthodox *trans*-addition mode. The well-balanced affinities of the different reaction partners to the ruthenium catalyst ensure that crossed addition prevails over homodimerization of the individual components, as can be deduced from spectroscopic and crystallographic data of various intermediates; this includes a dinuclear complex in which an internal alkyne bridges two [Cp*RuCl] fragments.

The addition of a terminal alkyne across an internal triple bond is a conceptually appealing yet highly challenging approach to 1,3-enynes (Scheme 1).[1,2] For such a hydroalkynylation reaction to become useful, competing homodimerization, oligomerization, and/or cyclotrimerization of either partner must be suppressed and regiocontrol be imposed when working with unsymmetrical substrates ($R^1 \neq R^2$). The stereochemical course of the reaction is usually less of an issue in that *cis*-hydroalkynylation is observed,[1,2] except for special cases: a notable exception employs biased N-sulfonyl ynamides, which resulted in net *trans*-hydroalkynylation.[3,4] Even more demanding are related halo-alkynylations.[5] The fact that the C−X bond of the resulting haloenyne product might react with the catalyst used for its preparation poses an additional challenge; unsurprisingly, perhaps, the few known examples uniformly follow a *cis*-addition mode.[6]

Scheme 1. Challenge of Crossed Hydro(chloro)alkynylation

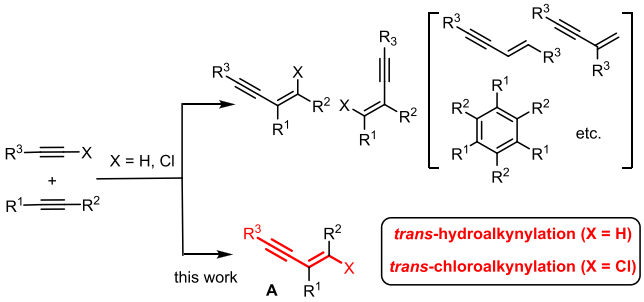

Outlined below are an efficient *trans*-hydroalkynylation of unbiased internal alkynes and the first *trans*-chloroalkynylation reactions ever. Since 1,3-enynes in general serve as valuable building blocks,[1,2] the new entry is enabling. This is particularly true for chloroenynes of type **A** (X = Cl), as they comprise adjacent electrophilic and nucleophilic sites amenable to orthogonal activation. Their dual reactivity can be harnessed in small-molecule synthesis and material science alike: the benzannulation strategy leading to polysubstituted arenes by cycloisomerization/cross-coupling (see below)[7,8] and the preparation of π-conjugated oligomers with valuable optoelectronic properties,[9] are deemed representative.

Following up on our investigations into ruthenium-catalyzed *trans*-hydrogenation[10,11] and *trans*-hydrometalation[12−19] catalyzed by $\{Cp^*RuCl\}_4$ or related complexes, we reasoned that the reactivity pattern manifested in these unorthodox transformations might be further extended.[20] For their activated C−H bonds, terminal alkynes were deemed promising candidates; the desirable "crossed" addition mode seemed possible because [Cp*RuCl] readily forms heteroleptic complexes comprising two different π-ligands.[21,22]

To test this hypothesis, various terminal alkynes were screened (see the SI), but only triisopropylsilylacetylene (**1a**) gave good results (Scheme 2).[23] In the presence of catalytic $[Cp^*RuCl]_4$, **1a** reacts with internal dialkylalkynes to form the corresponding *trans*-addition products; the *Z*:*E* ratios are generally excellent. The stereochemistry was assigned by NMR and confirmed for product **9** by X-ray diffraction (see the SI). As expected, the functional group tolerance is high, in that ketones, esters, unprotected alcohols, acetals, aryl and alkyl halides, as well as cyclopropyl rings, remain intact. Aromatic substrates, however, react less well, likely because [Cp*Ru] tends to form kinetically stable η^6-arene adducts that may sequester the catalyst (cf. **6**; for further examples, see the SI); this limitation has precedent in the *trans*-hydroelementation reactions cited above.[10−20]

Unsymmetrical substrates usually afford mixtures of regioisomers (see the SI), but propargyl alcohols of type **10** provide a handle to control the outcome (Table 1): $[Cp^*RuCl]_4$ favors "proximal delivery" to give the α-*trans*

Received: August 10, 2020
Published: October 23, 2020

https://dx.doi.org/10.1021/jacs.0c08582
J. Am. Chem. Soc. 2020, 142, 18746−18752

Scheme 2. *trans*-Hydroalkynylation

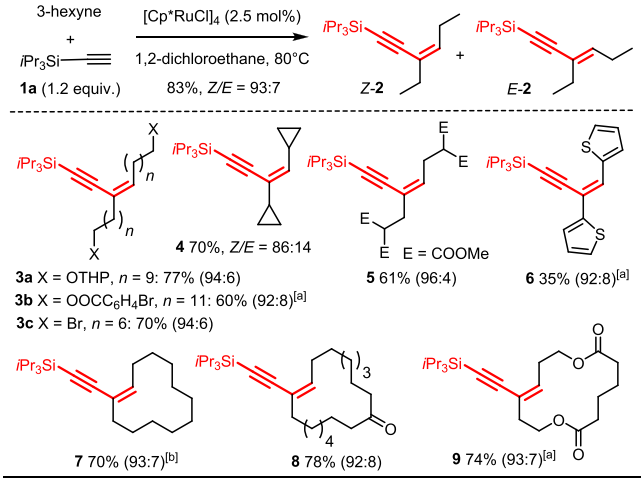

[a]5 mol% of catalyst. [b]NMR yield.

Table 1. Catalyst-Dependent Regioselectivity

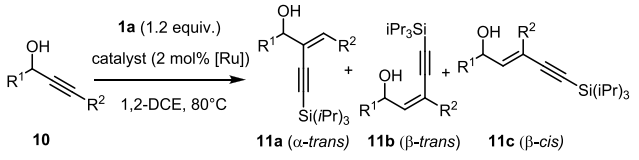

Nr	Catalyst	R^1, R^2	Yield (%)	**11a:b:c**
1	$[Cp^*Ru(MeCN)_3]SbF_6$	Me, Me	66	10:59:31
2	$[Cp^*Ru(MeCN)_3]SbF_6$[a]	Me, Me	76	75:10:15
3	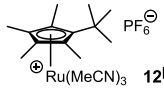 **12**[a]	Me, Me	84	84:10:6
4	$[Cp^*RuCl]_4$	Me, Me	84	74:10:16
5	$[Cp^*RuCl]_4$	Et, Me	82	72:10:16[b]
6	$[Cp^*RuCl]_4$	Me, C_8H_{17}	62	83:11:6
7	$[Cp^*RuCl]_4$	H, Pr	65	65:6:0[b]

[a]In the presence of nBu$_4$NCl (10 mol%). [b]The remainder is the *α-cis* isomer.

addition product, whereas cationic $[Cp^*Ru(MeCN)_3]SbF_6$ leads to the regio-complementary outcome, although the overall selectivity is lower. As previously shown for analogous *trans*-hydrometalations, proximal delivery is caused by interligand hydrogen bonding between the [Ru-Cl] group and the propargylic −OH substituent.[18,19] The selectivity can be further improved by using the bulkier complex **12** in combination with nBu$_4$NCl,[24] even though the reaction proceeds more slowly. This result holds the promise that more systematic ligand tuning will allow for further optimization.

At this point, however, the search for yet other substrates amenable to *trans*-addition was given priority. Gratifyingly, (chloroethynyl)triisopropylsilane (**1b**) also reacts well, resulting in *trans*-chloroalkynylation of internal alkyne partners (Scheme 3);[25,26] to the best of our knowledge, this transformation is unprecedented and the selectivity remarkably high. The stereochemical outcome was ascertained by NMR (see the SI). The structure of **21** in the solid state confirmed the assignment (Figure 1).[27]

Scheme 3. *trans*-Chloroalkynylation of Symmetrical Alkynes[a]

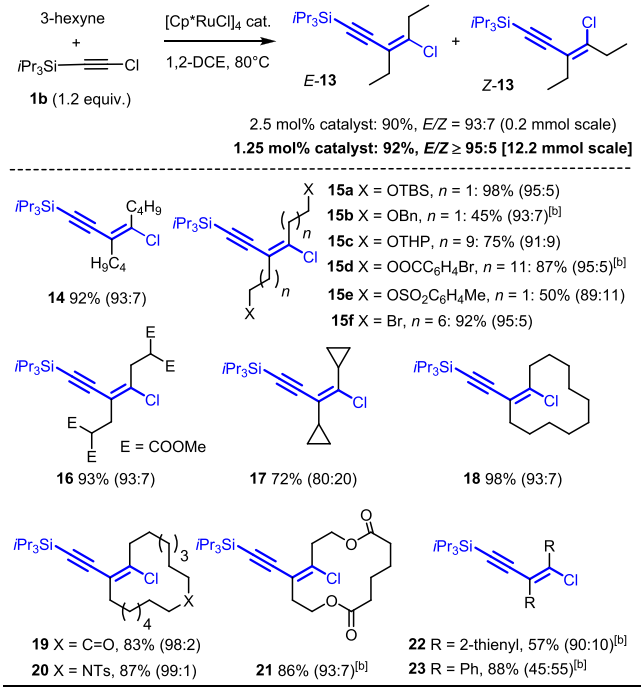

[a]2.5 mol% catalyst, unless stated otherwise. [b]5 mol% catalyst.

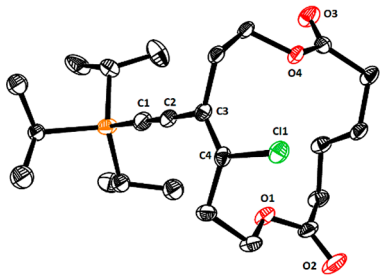

Figure 1. Structure of compound **21** in the solid state. Thermal ellipsoids at the 50% probability level.[27]

The scope is significantly broader than that of the *trans*-hydroalkynylation in that good results were obtained in many cases even for aromatic and/or unsymmetrical substrates (Scheme 4). This is particularly true for propynylated arenes, which gave excellent yields and notably high *E*/*Z*-ratios, independent of whether electron-withdrawing or -donating substituents were placed on the aromatic ring. Likewise, propynylated pyridine or thiophene reacted well despite the heteroatom donor sites. Tolane, in contrast, was the only alkyne investigated so far in which *cis*-chloroalkynylation was truly competitive (**23**, *E*:*Z* = 45:55). Collectively, these examples illustrate the scope and notable functional group compatibility of the reaction, which matches the experiences previously made with various other ruthenium-catalyzed *trans*-addition processes.[20]

The *trans*-chloroalkynylation of 3-hexyne was also carried out on 12.2 mmol scale with a reduced catalyst loading of 1.25 mol%. While the yield of **13** remained unchanged (92%),[28] the *E*/*Z*-ratio was slightly improved (≥95:5 versus 93:7 at 2.5 mol % $[Cp^*RuCl]_4$); this observation is consistent with the mechanistic insights outlined below. Likewise, chloroenyne

https://dx.doi.org/10.1021/jacs.0c08582
J. Am. Chem. Soc. 2020, 142, 18746−18752

Scheme 4. *trans*-Chloroalkynylation of Unsymmetrical Alkynes[a]

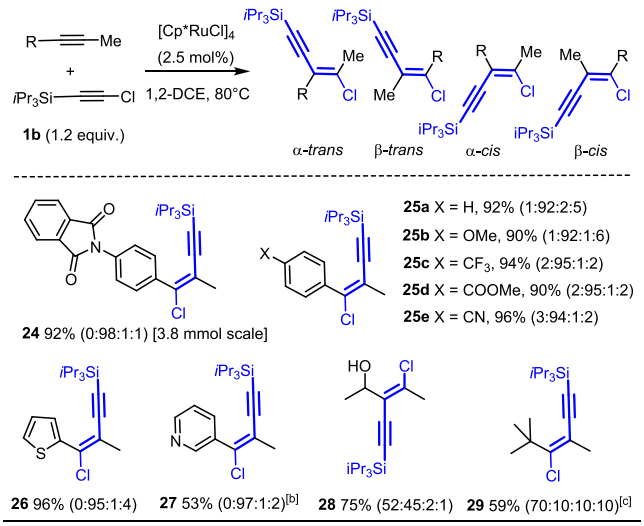

[a]Only the major product isomer is shown (isomer ratio). [b]5 mol% catalyst. [c]NMR yield.

24 was formed on gram scale; after recrystallization, the material was almost isomerically pure.

The chloroalkenes thus formed are relevant in that they bring stereodefined tetrasubstituted alkenes into reach, as illustrated by the iron-catalyzed formation of the polyfunctionalized product **30** (Scheme 5).[29] The π-acid-catalyzed cycloisomerization of **31** derived from **25c** showcases a very different application: Catalytic $PtCl_2$ affords the corresponding naphthalene derivative **32**, retaining a chloride substituent for further manipulation;[30,31] its iron-catalyzed borylation with

Scheme 5. Downstream Functionalization

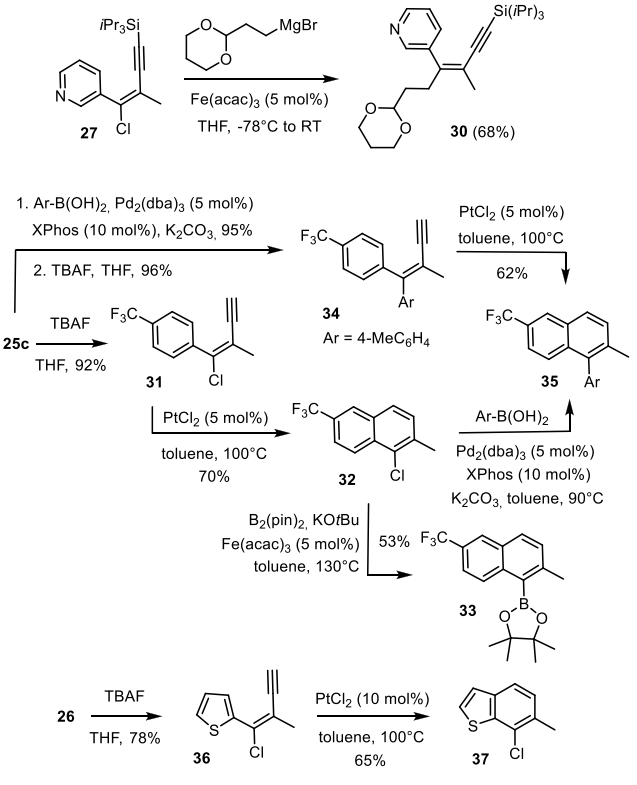

formation of **33** represents just one such possibility.[32] The many other ways of engaging a halide into all sorts of cross-coupling bring innumerous arene derivatives into reach with substitution patterns that are difficult to make otherwise.[33,34] Equally important is the fact that the concept underlying this new benzannulation is also applicable to the heterocyclic series, as illustrated by the formation of chlorobenzothiophene **37**. Further flexibility is gained by the possibility of interchanging the order of cycloisomerization/cross-coupling, as demonstrated by the two sequences leading to **35**. These enabling virtues are subject to further study.

The fact that the "crossed" addition prevails over homodimerization (oligomerization) of either reaction partner speaks for a well-orchestrated coordination chemistry, especially since neither substrate has to be used in large excess. To gain insights, we first studied the interaction of the individual components with the catalyst (Scheme 6). Addition

Scheme 6. Reactive Intermediates

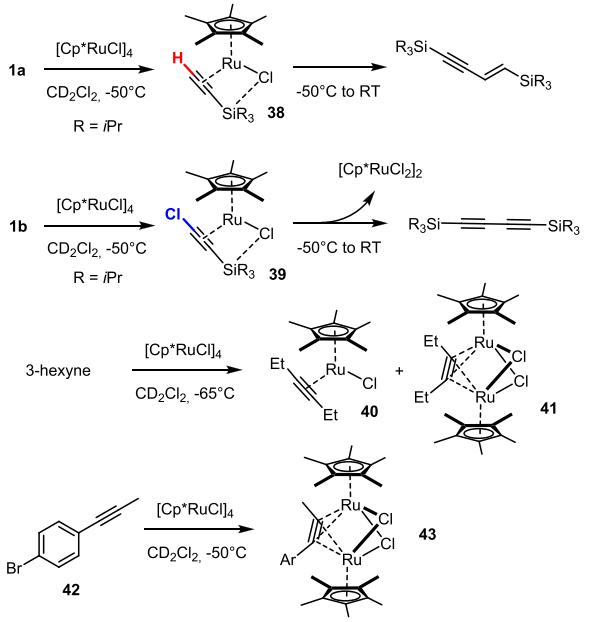

of $[Cp^*RuCl]_4$ (0.25 equiv) to **1a** in CD_2Cl_2 at −50 °C leads to a cherry-red solution containing some unbound **1a** and a single new species. Based on the diagnostic deshielding of the alkyne C-atoms (135.7/137.5 ppm; compare: 85.9/94.8 ppm in **1a**) and the "olefinic" character of the alkyne proton (δ_H = 8.64 ppm; compare 2.43 ppm in **1a**), this species can be safely assigned as the corresponding π-complex **38**.[18,19] Its structure in the solid state (Figure 2) shows the substantial elongation of the C1−C2 (1.265(3) Å)[35] bond, together with the notable bending of the alkyne away from linearity (H1−C1−C2 144.5(4)°; C1−C2−Si1 153.0(2)°) as the result of substantial electron back-donation from the filled metal d-orbitals into the π^*-orbitals of the bound alkyne.[19] The silyl group is oriented toward the chlorine ligand, which is favorable on steric as well as electronic grounds:[36] attractive interligand interactions between a polarized [Ru-Cl] unit and a silyl substituent have previously been invoked to explain the outcome of various mechanistically different transformations.[18,19,37] The fact that only a single molecule of **1a** is coordinated to the 14-electron fragment [Cp*RuCl] is of particular relevance, as it leaves a vacant site for uptake of the reaction partner as necessary for

https://dx.doi.org/10.1021/jacs.0c08582
J. Am. Chem. Soc. 2020, 142, 18746−18752

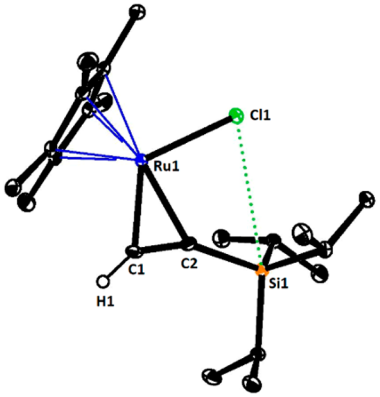

Figure 2. Structure of **38** in the solid state; thermal ellipsoids at the 50% probability level. The dotted green line indicates an attractive interligand interaction between the [Ru-Cl] unit and the silyl group.[36]

crossed addition.[38] It is here that the size of the TIPS group is thought to come into play: slim $Me_3SiC{\equiv}CH$ in lieu of **1a** is rapidly consumed by homocyclodimerization[39] and is therefore no suitable substrate for *trans*-hydroalkynylation. Although **1a** will eventually also homodimerize upon warming, the reaction is slow enough to leave the desired crossed addition time to proceed.

Chloroalkyne **1b** shows a similar coordination behavior, as indicated by the massive downfield shifts of the alkyne C-atoms (141.1/150.6 ppm; compare: 70.9/79.5 ppm in **1b**). Complex **39** also comprises only one alkyne ligand (Figure 3),

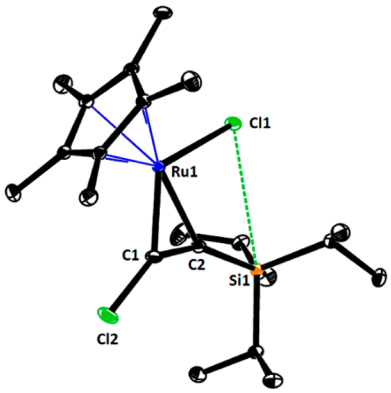

Figure 3. Structure of **39** in the solid state; thermal ellipsoids at the 50% probability level. The dotted line indicates an attractive interligand interaction.[40] Selected bond lengths (Å) and angles (deg): C1−C2 1.279(2), C1−Cl2 1.70(1), Cl2−C1−C2 141.4(5), C1−C2−Si1 152.7(1).

featuring the typical signs of partial rehybridization.[19,40] When a solution of this complex in CD_2Cl_2 is warmed from −50 °C to room temperature, slow decomposition with formation of the corresponding conjugated diyne and paramagnetic $[Cp^*RuCl_2]_2$[41] is observed.

In contrast, 3-hexyne as prototypical reaction partner for **1a**,**b** leads to two new signal sets when reacted with $[Cp^*RuCl]_4$ (0.25 equiv) at low temperature (Scheme 6). While one of them certainly corresponds to the corresponding monoalkyne complex **40**, the second species is a [2:1]-adduct in which two metal fragments ligate the same triple bond.[42] Single crystals of putative **41** could not be grown, but replacement of 3-hexyne by 1-bromo-4-(prop-1-yn-1-yl)-benzene was met with success. In the resulting dinuclear complex **43**, one massively elongated alkyne (C2−C3 1.332(5) Å) and the two chlorine atoms bridge the two Ru centers (Figure 4).[43,44]

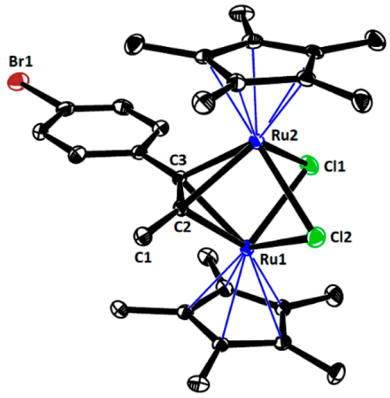

Figure 4. Structure of complex **43** in the solid state; thermal ellipsoids at the 50% probability level. Selected bond lengths (Å) and angles (deg): C2−C3 1.332(5), C1−C2−C3 147.2(4), C2−C3−C4 142.3(4).

With all individual complexes identified, a 1:1:1 mixture of $[Cp^*RuCl]_4$, chloroalkyne **1b**, and 3-hexyne was investigated with the hope of identifying the heteroleptic bis-alkyne complex resulting in crossed chloroalkynylation. When mixed at −50 °C in CD_2Cl_2, the hexyne-derived complexes **40** and **41** were the major species, whereas the chloroalkyne adduct **39** was minor. Upon gradual warming to room temperature, the speciation changes in that **40** and **41** disappear and **39** is the only complex left (product formation commences). Signs of a mixed complex have not be detected at any point. Re-cooling of the equilibrated sample to −50 °C does not restore the original product distribution. Therefore, we conclude that binding of 3-hexyne is kinetically favored, but the chloroalkyne complex **39** is thermodynamically more stable.

The finding that an ordinary alkyne can bind two catalyst fragments simultaneously raised the question as to whether complex **40** or the [2:1] adduct **41** accounts for product formation. Variable time normalization analysis[45] proved that the formation of the *trans*-chloroalkynylation product (*E*)-**13** is first-order in [Ru] (Figure 5, top), whereas the formation of the minor *cis*-isomer shows a second-order dependence (see SI Figure S28).[46] The unexpected finding that the *trans*- and the *cis*-addition follow different rate laws readily explains why the *E*/*Z*-ratio depends on the catalyst concentration (Figure 6). In this context we reiterate the observation made during scale-up that lowering of the catalyst loading improved the selectivity to ≥95:5; for comparison, the stoichiometric control experiment furnished **13** with a poor *E*/*Z*-ratio of 64:36.

Furthermore, the consumption of 3-hexyne and the formation of the *trans*-addition product **13** show first-order dependence on the concentration of complex **39**. Hence, **39** likely represents the resting state of the catalytic process before the turnover-limiting step (Figure 5, bottom).

Since a "loaded" complex carrying two different alkynes has not been observed experimentally, we are currently not in the position to rigorously exclude an outer-sphere process, in which only the chloroalkyne is activated by coordination to ruthenium and is then attacked by 3-hexyne. Although indirect

https://dx.doi.org/10.1021/jacs.0c08582
J. Am. Chem. Soc. 2020, 142, 18746−18752

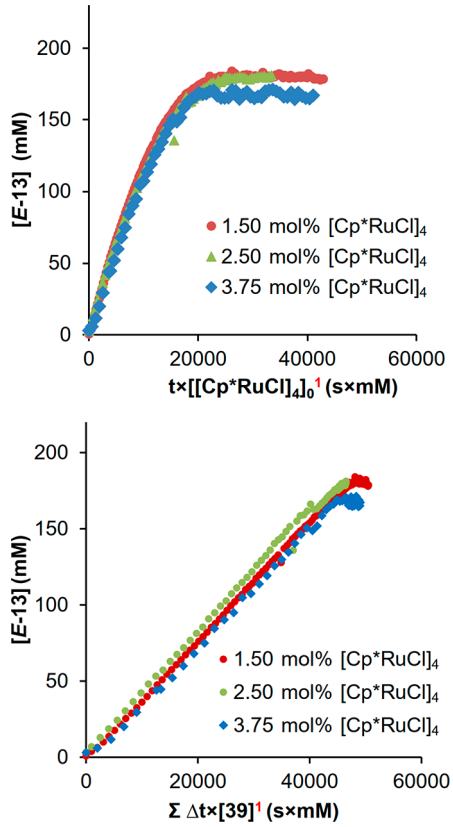

Figure 5. Variable time normalization analysis of NMR data. Formation of (*E*)-**13** shows first-order dependence in [Ru] (top) as well as in the chloroalkyne adduct **39** (bottom); in contrast, formation of (*Z*)-**13** shows second-order dependence in [Ru] (cf. Figure S28).

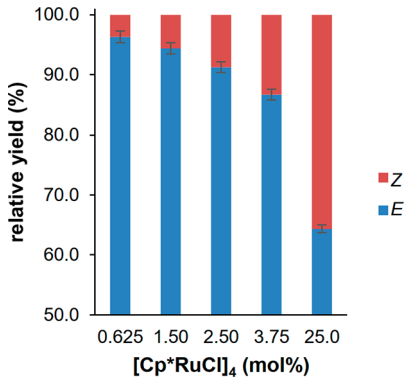

Figure 6. *E*/*Z*-ratio of **13** as a function of catalyst loading.

evidence speaks for an inner-sphere mechanism,[47] the final answer must await further study.

In summary, we demonstrate herein that ruthenium-catalyzed alkyne *trans*-addition chemistry can be expanded beyond *trans*-hydrogenation and *trans*-hydrometalations. The ease with which iPr$_3$SiC≡CX (X = H, Cl) add across internal alkynes in a highly selective *trans*-mode is remarkable and suggests that further extensions of this unorthodox reactivity paradigm might be possible.[48] This aspect is subject to ongoing studies in this laboratory.

■ ASSOCIATED CONTENT

Supporting Information

The Supporting Information is available free of charge at https://pubs.acs.org/doi/10.1021/jacs.0c08582.

Experimental section including characterization data, NMR spectra of new compounds, and supporting X-ray crystallographic data (PDF)
X-ray crystallographic data for **9** (CIF)
X-ray crystallographic data for **21** (CIF)
X-ray crystallographic data for **38** (CIF)
X-ray crystallographic data for **39** (CIF)
X-ray crystallographic data for **43** (CIF)

■ AUTHOR INFORMATION

Corresponding Author

Alois Fürstner − *Max-Planck-Institut für Kohlenforschung, 45470 Mülheim/Ruhr, Germany;* orcid.org/0000-0003-0098-3417; Email: fuerstner@kofo.mpg.de

Authors

Nagaraju Barsu − *Max-Planck-Institut für Kohlenforschung, 45470 Mülheim/Ruhr, Germany*

Markus Leutzsch − *Max-Planck-Institut für Kohlenforschung, 45470 Mülheim/Ruhr, Germany;* orcid.org/0000-0001-8171-9399

Complete contact information is available at: https://pubs.acs.org/10.1021/jacs.0c08582

Notes

The authors declare no competing financial interest.

■ ACKNOWLEDGMENTS

Generous financial support by the MPG is gratefully acknowledged. We thank the analytical departments of our Institute for excellent support, especially J. Rust and Prof. C. W. Lehmann for solving the X-ray structures, and J. Lingnau, P. Philipps, M. Kochius, and Dr. C. Farès for help with the configurational assignment of numerous samples by NMR.

■ REFERENCES

(1) Garcia-Garrido, S. E. In *Modern Alkyne Chemistry*; Trost, B. M., Li, C.-J, Eds.; Wiley-VCH: Weinheim, 2015; pp 301−334.

(2) (a) Trost, B. M.; Masters, J. T. Transition Metal-Catalyzed Couplings of Alkynes to 1,3-Enynes: Modern Methods and Synthetic Applications. *Chem. Soc. Rev.* **2016**, *45*, 2212−2238. (b) Zhou, Y.; Zhang, Y.; Wang, J. Recent Advances in Transition-Metal-Catalyzed Synthesis of Conjugated Enynes. *Org. Biomol. Chem.* **2016**, *14*, 6638−6650. (c) Bao, X.; Ren, J.; Yang, Y.; Ye, X.; Wang, B.; Wang, H. 2-Activated 1,3-Enynes in Enantioselective Synthesis. *Org. Biomol. Chem.* **2020**, DOI: 10.1039/D0OB01614D. (d) Yi, C. S.; Liu, N. Ruthenium-Catalyzed Coupling Reactions of Alkynes and Alkenes. *Synlett* **1999**, *1999*, 281−287.

(3) Liu, G.; Kong, W.; Che, J.; Zhu, G. Palladium-Catalyzed Cross Addition of Terminal Alkynes to Aryl Ynamides: An Unusual *trans*-Hydroalkynylation Reaction. *Adv. Synth. Catal.* **2014**, *356*, 3314−3318.

(4) For net *trans*-additions to propargyl alcohols or diarylalkynes using a strategy that avoids the use of terminal alkynes as partners, see: (a) Horita, A.; Tsurugi, H.; Funayama, A.; Satoh, T.; Miura, M. Regio- and Stereoselective Cross-Coupling of *tert*-Propargyl Alcohols with Bis(trimethylsilyl)acetylene and Its Utilization in Constructing a Fluorescent Donor-Acceptor System. *Org. Lett.* **2007**, *9*, 2231−2233. (b) Horita, A.; Tsurugi, H.; Satoh, T.; Miura, M. Rhodium-Catalyzed Anti Selective Cross-Addition of Bis(trimethylsilyl)acetylene to

Diarylacetylenes via Carbon-Silicon Bond Cleavage. *Org. Lett.* **2008**, *10*, 1751−1754.
(5) (a) Petrone, D. A.; Ye, J.; Lautens, M. Modern Transition-Metal-Catalyzed Carbon-Halogen Bond Formation. *Chem. Rev.* **2016**, *116*, 8003−8104. (b) Wu, W.; Jiang, H. Haloalkynes: A Powerful and Versatile Building Block in Organic Synthesis. *Acc. Chem. Res.* **2014**, *47*, 2483−2504.
(6) (a) Kreuzahler, M.; Haberhauer, G. Gold(I)-Catalyzed Haloalkynalytion of Aryl Alkynes: Two Pathways, One Goal. *Angew. Chem., Int. Ed.* **2020**, *59*, 9433−9437. (b) Wada, T.; Iwasaki, M.; Kondoh, A.; Yorimitsu, H.; Oshima, K. Palladium-Catalyzed Addition of Silyl-Substituted Chloroalkynes to Terminal Alkynes. *Chem. - Eur. J.* **2010**, *16*, 10671−10674. (c) Li, Y.; Liu, X.; Jiang, H.; Feng, Z. Expedient Synthesis of Functionalized Conjugated Enynes: Palladium-Catalyzed Bromoalkynylation of Alkynes. *Angew. Chem., Int. Ed.* **2010**, *49*, 3338−3341. See also: (d) Morishita, T.; Yoshida, H.; Ohshita, J. Copper-Catalysed Bromoalkynlation of Arynes. *Chem. Commun.* **2010**, *46*, 640−642.
(7) (a) Saito, S.; Yamamoto, Y. Recent Advances in the Transition-Metal Catalyzed Regioselective Approaches to Polysubstituted Benzene Derivatives. *Chem. Rev.* **2000**, *100*, 2901−2915. (b) Wessig, P.; Müller, G. The Dehydro-Diels-Alder Reaction. *Chem. Rev.* **2008**, *108*, 2051−2063.
(8) (a) Michelet, V.; Toullec, P. Y.; Genet, J.-P. Cycloisomerization of 1,n-Enynes: Challenging Metal-Catalyzed Rearrangements and Mechanistic Insights. *Angew. Chem., Int. Ed.* **2008**, *47*, 4268−4315. (b) Fürstner, A. Catalytic Carbophilic Activation: Catalysis by Platinum and Gold π-Acids. *Angew. Chem., Int. Ed.* **2007**, *46*, 3410−3449.
(9) For the use of building blocks closely related to **13**−**17**, which had to be prepared over several stoichiometric steps, in material science, see: (a) Pilzak, G. S.; van Lagen, B.; Hendrikx, C. J.; Sudhölter, E. J. R.; Zuilhof, H. Synthesis and Optical Properties of all-*trans*-Oligodiacetylenes. *Chem. - Eur. J.* **2008**, *14*, 7939−7950. (b) Takayama, Y.; Delas, C.; Muraoka, K.; Uemura, M.; Sato, F. Highly Practical and General Synthesis of Monodisperse Linear π-Conjugated Oligoenynes and Oligoenediynes with either *trans*- or *cis*-Olefin Configuration. *J. Am. Chem. Soc.* **2003**, *125*, 14163−14167.
(10) Radkowski, K.; Sundararaju, B.; Fürstner, A. A Functional-Group-Tolerant Catalytic *trans*-Hydrogenation of Alkynes. *Angew. Chem., Int. Ed.* **2013**, *52*, 355−360.
(11) Guthertz, A.; Leutzsch, M.; Wolf, L. M.; Gupta, P.; Rummelt, S. M.; Goddard, R.; Farès, C.; Thiel, W.; Fürstner, A. Half-Sandwich Ruthenium Carbene Complexes Link *trans*-Hydrogenation and *gem*-Hydrogenation of Internal Alkynes. *J. Am. Chem. Soc.* **2018**, *140*, 3156−3159.
(12) For pioneering studies into *trans*-hydrosilylation, see: (a) Trost, B. M.; Ball, Z. T. Markovnikov Alkyne Hydrosilylation Catalyzed by Ruthenium Complexes. *J. Am. Chem. Soc.* **2001**, *123*, 12726−12727. (b) Trost, B. M.; Ball, Z. T. Alkyne Hydrosilylation Catalyzed by a Cationic Ruthenium Complex: Efficient and General Trans Addition. *J. Am. Chem. Soc.* **2005**, *127*, 17644−17655. (c) Trost, B. M.; Ball, Z. T. Addition of Metalloid Hydrides to Alkynes: Hydrometallation with Boron, Silicon, and Tin. *Synthesis* **2005**, *2005*, 853−887.
(13) Lacombe, F.; Radkowski, K.; Seidel, G.; Fürstner, A. (*E*)-Cycloalkenes and (*E,E*)-Cycloalkadienes by Ring Closing Diyne or Enyne-yne Metathesis/Semi-Reduction. *Tetrahedron* **2004**, *60*, 7315−7324.
(14) Matsuda, T.; Kadowaki, S.; Yamaguchi, Y.; Murakami, M. Ruthenium-Catalyzed *trans*-Hydrogermylation of Alkynes: Formation of 2,5-Disubstituted Germoles through Double *trans*-Hydrogermylation of 1,3-Diynes. *Org. Lett.* **2010**, *12*, 1056−1058.
(15) Sundararaju, B.; Fürstner, A. A *trans*-Selective Hydroboration of Internal Alkynes. *Angew. Chem., Int. Ed.* **2013**, *52*, 14050−14054.
(16) Longobardi, L.; Fürstner, A. *trans*-Hydroboration of Propargyl Alcohol Derivatives and Related Substrates. *Chem. - Eur. J.* **2019**, *25*, 10063−10068.
(17) Rummelt, S. M.; Fürstner, A. Ruthenium-Catalyzed *trans*-Selective Hydrostannation of Alkynes. *Angew. Chem., Int. Ed.* **2014**, *53*, 3626−3630.
(18) Rummelt, S. M.; Radkowski, K.; Rosca, D.-A.; Fürstner, A. Interligand Interactions Dictate the Regioselectivity of *trans*-Hydrometalations and Related Reactions Catalyzed by [Cp*RuCl]. Hydrogen Bonding to a Chloride Ligand as a Steering Principle in Catalysis. *J. Am. Chem. Soc.* **2015**, *137*, 5506−5519.
(19) Rosca, D.-A.; Radkowski, K.; Wolf, L. M.; Wagh, M.; Goddard, R.; Thiel, W.; Fürstner, A. Ruthenium-Catalyzed Alkyne *trans*-Hydrometalation: Mechanistic Insights and Preparative Implications. *J. Am. Chem. Soc.* **2017**, *139*, 2443−2455.
(20) Fürstner, A. *trans*-Hydrogenation, *gem*-Hydrogenation, and *trans*-Hydrometalation of Alkynes: An Interim Report on an Unorthodox Reactivity Paradigm. *J. Am. Chem. Soc.* **2019**, *141*, 11−24.
(21) (a) Trost, B. M.; Frederiksen, M. U.; Rudd, M. T. Ruthenium-Catalyzed Reactions—A Treasure Trove of Atom-Economic Transformations. *Angew. Chem., Int. Ed.* **2005**, *44*, 6630−6666.
(22) Rummelt, S. M.; Cheng, G.-J.; Gupta, P.; Thiel, W.; Fürstner, A. Hydroxy-Directed Ruthenium-Catalyzed Alkene/Alkyne Coupling: Increased Scope, Stereochemical Implications, and Mechanistic Rationale. *Angew. Chem., Int. Ed.* **2017**, *56*, 3599−3604;Corrigendum: *Angew. Chem., Int. Ed.* **2017**, *56*, 5652.
(23) For use of silylated alkynes in *cis*-selective hydroalkynylations of internal alkynes, see the following for leading references and literature cited therein: (a) Yi, C. S.; Liu, N. The Ruthenium Acetylide Catalyzed Cross-Coupling Reaction of Terminal and Internal Alkynes: Isolation of as Catalytically Active β-Agostic Intermediate Species. *Organometallics* **1998**, *17*, 3158−3160. (b) Katagiri, T.; Tsurugi, H.; Funayama, A.; Satoh, T.; Miura, M. Rhodium-Catalyzed Selective Cross-Coupling of Internal Alkynes with Terminal Silylacetylene. *Chem. Lett.* **2007**, *36*, 830−831. (c) Tsukada, N.; Ninomiya, S.; Aoyama, Y.; Inoue, Y. Palladium-Catalyzed Selective Cross-Addition of Triisopropylsilylacetylene to Internal and Terminal Unactivated Alkynes. *Org. Lett.* **2007**, *9*, 2919−2921. (d) Nishimura, T.; Guo, X.-X.; Ohnishi, K.; Hayashi, T. Rhodium-Catalyzed Hydroalkynylation of Internal Alkynes with Silylacetylenes: An Alkynylrhodium(I) Intermediate Generated from the Hydroxyorhodium(I) Complex $[Rh(OH)(binap)]_2$. *Adv. Synth. Catal.* **2007**, *349*, 2669−2672. (e) Ito, J.; Kitase, M.; Nishiyama, H. Cross-Coupling of Alkynes Catalyzed by Phebox-Rhodium Acetate Complexes. *Organometallics* **2007**, *26*, 6412−6417. (f) Matsuyama, N.; Tsurugi, H.; Satoh, T.; Miura, M. Ligand-Controlled Cross-Dimerization and -Trimerization of Alkynes under Nickel Catalysis. *Adv. Synth. Catal.* **2008**, *350*, 2274−2278. (g) Sakurada, T.; Sugiyama, Y.; Okamoto, S. Cobalt-Catalyzed Cross Addition of Silylacetylenes to Internal Alkynes. *J. Org. Chem.* **2013**, *78*, 3583−3591.
(24) Biberger, T.; Gordon, C.; Leutzsch, M.; Peil, S.; Guthertz, A.; Copéret, C.; Fürstner, A. Alkyne *gem*-Hydrogenation: Formation of Pianostool Ruthenium Carbene Complexes and Analysis of Their Chemical Character. *Angew. Chem., Int. Ed.* **2019**, *58*, 8845−8850.
(25) Other chloroalkynes were unsuitable; see the SI. However, $i Pr_3SiC{\equiv}CX$ (X = Br, I) react but lead to partial halide scrambling with incorporation of chloride from the catalyst and/or the solvent.
(26) For a remotely related *trans*-addition of HCl catalyzed by [Cp*Ru] complexes, see: Dérien, S.; Klein, H.; Bruneau, C. Selective Ruthenium-Catalyzed Hydrochlorination of Alkynes: One-Step Synthesis of Vinylchlorides. *Angew. Chem., Int. Ed.* **2015**, *54*, 12112−12115.
(27) Figure 1 unmistakably shows the *trans*-arrangement of the chloride and the alkyne substituent on the tetrasubstituted double bond. Because the sample used for crystallization was prepared using (bromoethynyl)triisopropylsilane in 1,2-dichloroethane, partial incorporation of bromine and chlorine over the same position is observed, cf. ref 25; only the chlorine-containing product is shown for clarity
(28) Loadings <1 mol% tend to lead to incomplete conversion.

https://dx.doi.org/10.1021/jacs.0c08582
J. Am. Chem. Soc. 2020, 142, 18746−18752

(29) Fürstner, A.; Leitner, A.; Méndez, M.; Krause, H. Iron-Catalyzed Cross-Coupling Reactions. *J. Am. Chem. Soc.* **2002**, *124*, 13856−13863.
(30) Mamane, V.; Hannen, P.; Fürstner, A. Synthesis of Phenanthrenes and Polycyclic Heteroarenes by Transition-Metal Catalyzed Cycloisomerization Reactions. *Chem. - Eur. J.* **2004**, *10*, 4556−4575.
(31) Kang, D.; Kim, J.; Oh, S.; Lee, P. H. Synthesis of Naphthalenes via Platinum-Catalyzed Hydroarylation of Aryl Enynes. *Org. Lett.* **2012**, *14*, 5636−5639.
(32) Yoshida, T.; Ilies, L.; Nakamura, E. Iron-Catalyzed Borylation of Aryl Chlorides in the Presence of Potassium *t*-Butoxide. *ACS Catal.* **2017**, *7*, 3199−3203.
(33) Toyota, S.; Iwanaga, T. Naphthalenes, Anthracenes, 9*H*-Fluorenes, and Other Acenes. *Science of Synthesis* **2010**, *45*, 745−854.
(34) For a very different recent entry into 1-chloronaphthalene derivatives and summary of pertinent literature on their functionalization and use, see: Moriguchi, K.; Kono, T.; Seko, S.; Tanabe, Y. Gram-Scale Robust Synthesis of 1-Chloro-2,3-dimethyl-4-phenylnaphthalene: A Promising Scaffold with Three Contiguous Reaction Positions. *Synthesis* **2020**, DOI: 10.1055/s-0040-1706471.
(35) The corresponding bond length in $Me_3SiC{\equiv}CH$ is 1.200 Å, cf.: Bond, A. D.; Davies, J. E. Trimethylsilylacetylene. *Acta Crystallogr., Sect. E: Struct. Rep. Online* **2002**, *58*, o777.
(36) The Cl1···Si1 (3.53 Å) distance is well below the sum of the van der Waals radii of these atoms (4.22 Å), and the C−Si−C angles slightly deviate from the ideal tetrahedral geometry (106.2, 111.1, 112.9°); moreover, the distances between Cl and the H-atoms directed toward it are notably short (2.7−3.1 Å; sum of van der Waals radii: 3.6 Å) and are likely stabilizing, too.
(37) Gutsulyak, D. V.; Churakov, A. V.; Kuzmina, L. G.; Howard, J. A. K.; Nikonov, G. I. Steric and Electronic Effects in Half-Sandwich Ruthenium Silane σ-Complexes with Si-H and Si-Cl Interligand Interactions. *Organometallics* **2009**, *28*, 2655−2657.
(38) This notion is supported by a crystallographically and spectroscopically fully characterized complex, in which a [Cp*Ru(Cl)(η^2-alkyne) fragment ligates a tethered alkene at the former "open" coordination site"; see ref 22.
(39) See the following reference which corrects earlier literature: Gemel, C.; LaPensée, A.; Mauthner, K.; Mereiter, K.; Schmid, R.; Kirchner, K. The Substitution Chemistry of RuCp*(tmeda)Cl. *Monatsh. Chem.* **1997**, *128*, 1189−1199.
(40) Again, the short contact between the TIPS group and the [Ru-Cl] unit in **39** speaks for an attractive interligand interaction: as for complex **38** (see ref 36), the Cl1···Si1 (3.45 Å) distance as well as the distances between Cl and the H-atoms directed toward it (3.04−3.13 Å) are notably short; in this case, however, the C−Si−C angles deviate only slightly from the ideal tetrahedral geometry (105.1, 110.1, 110.5°).
(41) Identified by comparison with an authentic sample; for details, see the SI.
(42) This composition was suggested by the integrals over the ^{1}H NMR signals; at ≥0 °C, the monomeric and the dimeric complexes are in exchange on the NMR time scale.
(43) The closest analogue to **43** is a triruthenium cluster, in which trimethylsilylacetylene bridges two of the three metal atoms in a similar manner, serving as a 4e-donor ligand. See: Campion, B. K.; Heyn, R. H.; Tilley, T. D. Reactions of Alkynes with Coordinatively Unsaturated (η^5-C_5Me_5)Ru Derivatives. X-ray Crystal Structures of (η^5-C_5Me_5)Cl_2Ru(η^2:η^4-μ_2-C_4H_4)Ru(η^5-C_5Me_5) and (η^5-C_5Me_5)$_3Ru_3$(μ_2-Cl)(μ_3-Cl)(η^2-μ_2-HC≡CSiMe_3). *Organometallics* **1990**, *9*, 1106−1112.
(44) Another binuclear complex was observed, likely as a byproduct, in *trans*-additions to 1,3-diyne substrates; in this case, one of the Cp* rings was transformed into a fulvene by interligand hydride transfer. See: Mo, X.; Letort, A.; Rosca, D.-A.; Higashida, K.; Fürstner, A. Site-Selective *trans*-Hydrostannation of 1,3- and 1,n-Diynes: Application to the Total Synthesis of Typhonosides E and F, and a Fluorinated Cerebroside Analogue. *Chem. - Eur. J.* **2018**, *24*, 9667−9674.
(45) (a) Burés, J. A Simple Graphical Method to Determine the Order in Catalyst. *Angew. Chem., Int. Ed.* **2016**, *55*, 2028−2031. (b) Burés, J. Variable Time Normalization Analysis: General Graphical Elucidation of Reaction Orders from Concentration Profiles. *Angew. Chem., Int. Ed.* **2016**, *55*, 16084−16087.
(46) Deviations were observed at low loading (0.625 mol%), which is attributed to partial degradation of the catalyst. Compare: Martínez-Carrión, A.; Howlett, M. G.; Alamillo-Ferrer, C.; Clayton, A. D.; Bourne, R. A.; Codina, A.; Vidal-Ferran, A.; Adams, R. W.; Burés, J. *Angew. Chem., Int. Ed.* **2019**, *58*, 10189−10193. This observation inspired the variable time normalization analysis with regard to [**39**] where all lines (including the one based on 0.625% loading) overlap when assuming first-order-dependence; see the SI.
(47) The fact that a propargylic −OH group exerts a directing effect most likely via Ru-Cl···HO− interligand hydrogen bonding speaks for coordination of both reaction partners to the Ru-center, cf. Table 1; this steering effect mirrors the results of *trans*-hydrosilylation (stannylation), which has been shown by a combined experimental and computational approach to be an inner-sphere process. Cf. refs 18 and 19.
(48) For recent forays into *trans*-carboboration, see the following and literature cited therein: Jin, H.; Fürstner, A. Modular Synthesis of Furans with up to Four Different Substituents by a *trans*-Carboboration Strategy. *Angew. Chem., Int. Ed.* **2020**, *59*, 13618−13622.

https://dx.doi.org/10.1021/jacs.0c08582
J. Am. Chem. Soc. 2020, 142, 18746−18752